Two polymeric structures with a benzene-1,2,4,5-tetracarboxylate ligand acting in μ_2- and μ_4-bridging modes

Ana María Atria,[a] Gino Corsini,[b] Lissette González,[a,b] Maria Teresa Garland[c] and Ricardo Baggio[d]*

[a]Facultad de Ciencias Químicas y Farmacéuticas, Universidad de Chile, Casilla 233, Santiago, Chile, [b]Laboratorio de Bacteriología Molecular, Facultad de Ciencias de la Salud, Universidad Diego Portales, Santiago, Chile, [c]Departamento de Física, Facultad de Ciencias Físicas y Matemáticas and CIMAT, Universidad de Chile, Santiago de Chile, Chile, and [d]Departamento de Física, Centro Atómico Constituyentes, Comisión Nacional de Energía Atómica, Buenos Aires, Argentina
Correspondence e-mail: baggio@cnea.gov.ar

catena-Poly[[tetraaquabis(1*H*-pyrazole-κN^2)nickel(II)] [[diaquabis(1*H*-pyrazole-κN^2)nickel(II)]-μ-benzene-1,2,4,5-tetra-carboxylato-$\kappa^2 O^1 : O^4$] tetrahydrate], {[Ni(C$_3$H$_4$N$_2$)$_2$(H$_2$O)$_4$]-[Ni(C$_{10}$H$_2$O$_8$)(C$_3$H$_4$N$_2$)$_2$(H$_2$O)$_2$]·4H$_2$O}$_n$, (I), and poly[[(μ_4-benzene-1,2,4,5-tetracarboxylato-$\kappa^4 O^1 : O^2 : O^4 : O^5$)octakis(1*H*-pyrazole-$\kappa N^2$)dicobalt(II)] tetrahydrate], {[Co$_2$(C$_{10}$H$_2$O$_8$)-(C$_3$H$_4$N$_2$)$_8$]·4H$_2$O}$_n$, (II), are polymeric compounds crystallizing in the space group $P\bar{1}$, with two independent metallic cations and one benzene-1,2,4,5-tetracarboxylate (btc) anion, each lying on symmetry centres. Individual coordination polyhedra are regular and the main differences are in the way the btc anion binds [μ_2 in (I) and μ_4 in (II)], promoting a 'chain-like' one-dimensional structure in (I) and a 'sieve-like' two-dimensional motif in (II).

Comment

The study of one-, two- or three-dimensional molecular systems based on carboxylate-bridged metal centres is attractive not only due to their usually interesting structural characteristics (Eddaoudi *et al.*, 2001) but also for their potential applications, *viz.* in heterogeneous catalysis, medicine or chemical separation, and, on occasion, due to their eventual electronic and/or magnetic properties (Yaghi *et al.*, 1996; Ait-Haddou *et al.*, 2004).

In the synthesis of these systems, several factors are of relevance, namely the characteristics of the organic ligands, such as bridging capacity, shape, functionality, flexibility, *etc.* (Tudor *et al.*, 2003; Kooijman *et al.*, 2004), the noncovalent interactions which they might eventually give rise to, *viz.* hydrogen bonding, π–π interactions, *etc.* (Perron *et al.*, 2004), and, obviously, the nature of the metal ion.

The dramatic effect of this latter factor is apparent in the title complexes, [Ni(pyr)$_2$(H$_2$O)$_4$]$^{2+}$·[Ni(btc)(pyr)$_2$(H$_2$O)$_2$]$^{2-}$·4H$_2$O (btc is benzene-1,2,4,5-tetracarboxylate and pyr is pyrazole), (I), and Co$_2$(btc)(pyr)$_8$·4H$_2$O, (II), where absolute similarity in synthetic procedures, reaction conditions and reactant characteristics (containing closely related, but not identical, metal cations) nevertheless results in different compounds, both at a molecular and at a crystal structure level.

(I)

(II)
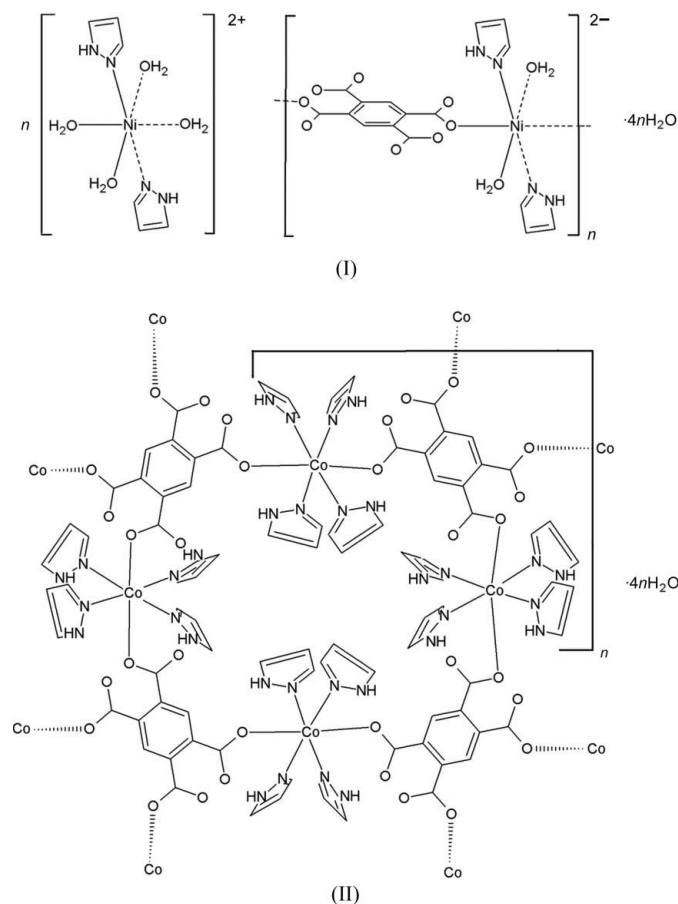
Figs. 1 and 2 show molecular views of (I) and (II), respectively. Tables 1 and 3, in turn, give some selected coordination parameters, and Tables 2 and 4 provide the hydrogen-bonding interactions. Even though both structures are polymeric and crystallize in the triclinic space group $P\bar{1}$, with two octahedral metal centres and one btc ligand occupying special positions on non-equivalent symmetry centres, this is basically the only common feature they share.

Compound (I) is ionic, with two well differentiated centrosymmetric substructures, *viz.* {[Ni(btc)(pyr)(H$_2$O)$_2$]$^{2-}$}$_n$ and n[Ni(pyr)$_2$(H$_2$O)$_4$]$^{2+}$. The Ni centre in each of these ionic units displays a rather regular octahedral environment, with mean coordination distances Ni—O = 2.085 (3) and 2.068 (9) Å, and Ni—N = 2.070 (3) and 2.068 (3) Å, and extreme values for the *cis* coordination angles of 90±3.82 (8) and 90±2.62 (10)° for atoms Ni1 and Ni2, respectively.

In (II), instead, both Co centres present one and the same Co(O$_{btc}$)$_2$(N$_{pyr}$)$_4$ coordination but with comparable regularity
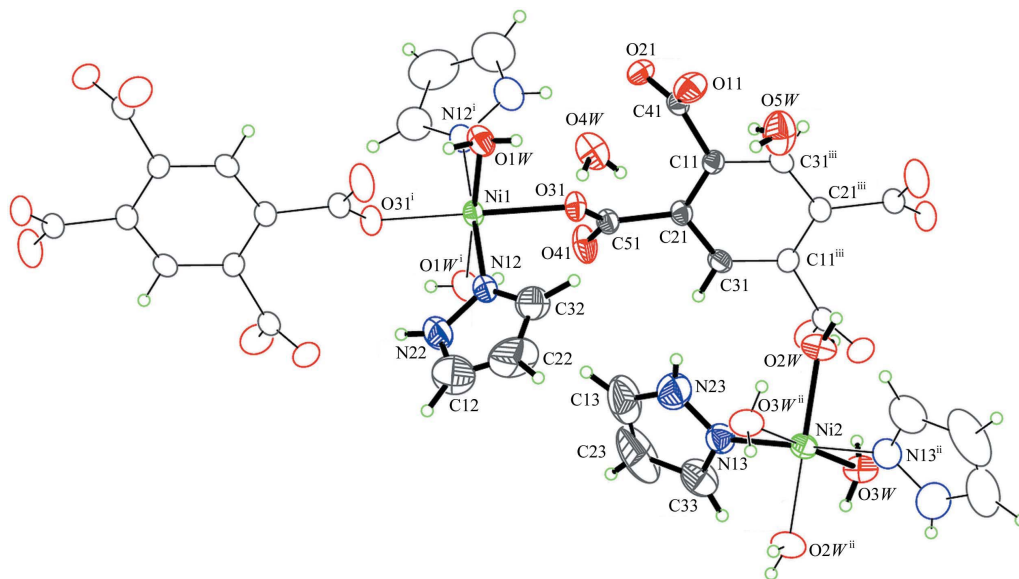
Figure 1

A molecular view of (I), showing the atom-numbering scheme. Displacement ellipsoids are drawn at the 50% probability level and H atoms are shown as small spheres of arbitrary radii. The asymmetric unit is shown in bold. [Symmetry codes: (i) $-x$, $1 - y$, $2 - z$; (ii) $-x + 1$, $-y$, $-z + 1$; (iii) $-x$, $-y + 1$, $-z + 1$.]

in the mean coordination distances of Co—O = 2.133 (3) and 2.070 (2) Å, and Co—N = 2.070 (3) and 2.120 (7) Å, and extreme values for the *cis* coordination angles of 90±4.87 (9) and 90±2.03 (9)° for atoms Co1 and Co2, respectively.
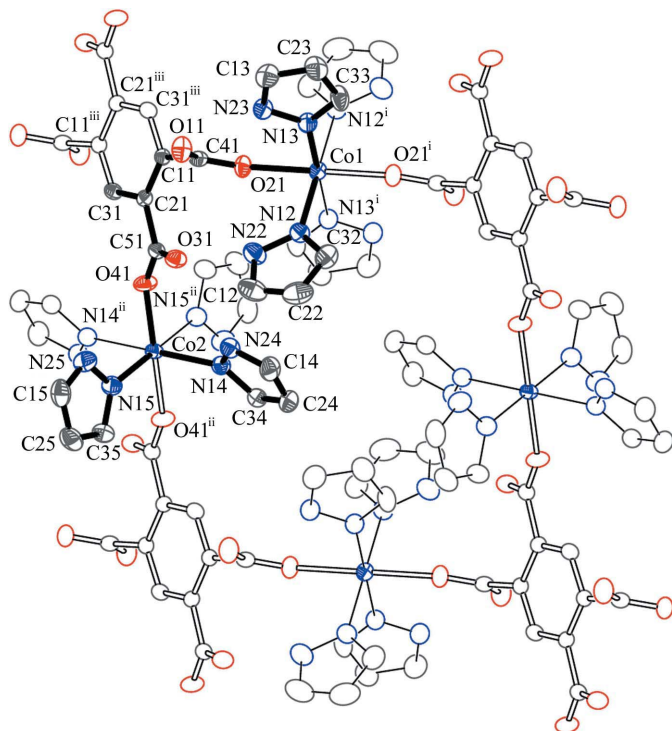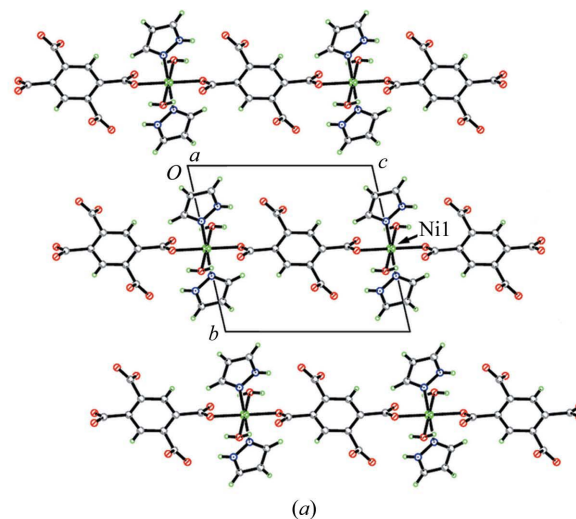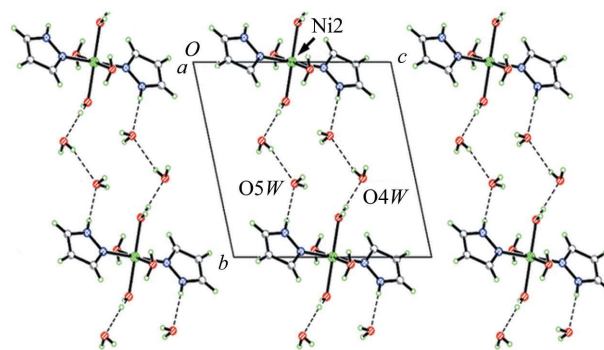

Figure 2

A molecular view of (II), showing the atom-numbering scheme. Displacement ellipsoids are drawn at the 50% probability level and H atoms are shown as small spheres of arbitrary radii. The asymmetric unit is shown in bold. [Symmetry codes: (i) $-x$, $1 - y$, $2 - z$; (ii) $-x$, $-y + 2$, $-z + 1$; (iii) $-x$, $-y + 1$, $-z + 1$.]
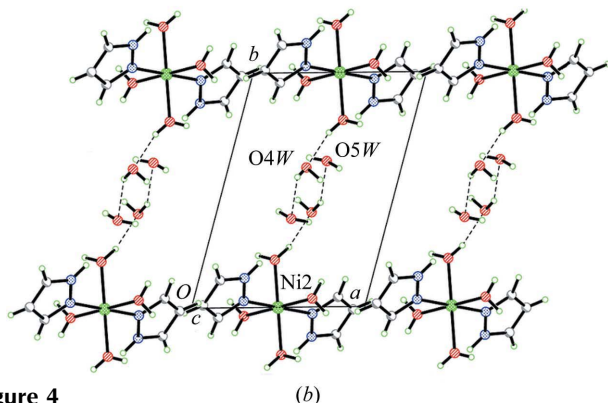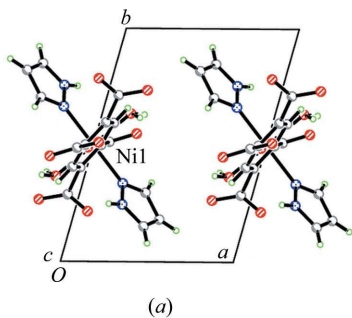

Figure 3

Packing view of (I), projected down [100]*. (*a*) At height $x = 0.00$, showing the (covalent) anionic chains running along [001], and (*b*) at height $x = \frac{1}{2}$, showing the (hydrogen-bonded) cationic chains running along [010].
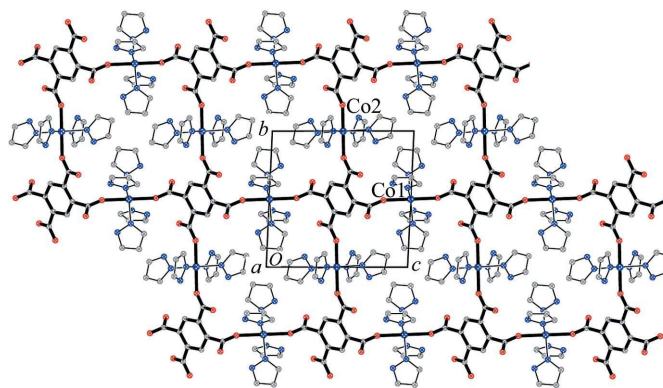
Figure 4
Packing view of (I), projected down [001]*. (a) At height z = 0.00, showing a cross-section of the (covalent) anionic chains running along [001] (out of the figure), and (b) at height $z = \frac{1}{2}$, showing the (hydrogen-bonded) cationic chains running along [010], in between the former chains.

Figure 5
Packing view of (II), projected down [100]*, showing (in bold) the 'grid structure' generated by Co^{II} cations and btc anions.

Figure 6
Packing view of (II), projected down [010]*, showing the water-mediated hydrogen-bond interaction between two-dimensional 'grid structures' (in bold).

As already stated, the btc anion in both structures lies on a centre of symmetry and, even though it acts as the bridging agent in both cases, it does so in two quite different ways, binding in a μ_2-bidentate fashion in Ni compound (I) and in a μ_4-tetradentate way in Co compound (II). This results in dramatic differences in both structural dimensionality and packing behaviour.
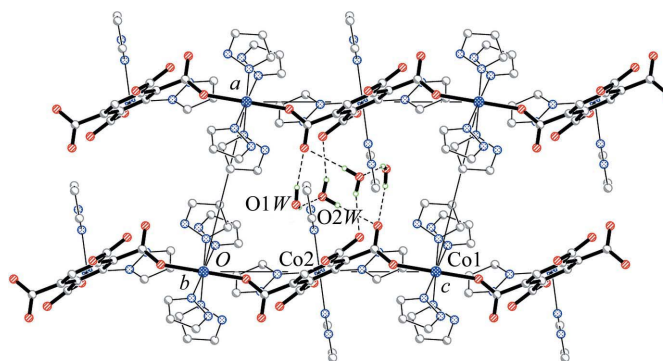
In (I), the simple bridging of the [Ni(pyr)$_2$(H$_2$O)$_4$]$^{2+}$ groups *via* the btc^{4-} anions generates negatively charged chains parallel to [001] containing only one of the two independent Ni atoms, *viz*. Ni1 (Fig. 3a). Atom Ni2 is involved in the formation of isolated [Ni(pyr)$_2$(H$_2$O)$_4$]$^{2+}$ cationic groups which form hydrogen-bonded chains perpendicular to the first set, which balance the charges (see discussion below and Fig. 3b).

The larger connectivity of the anion in (II) determines a two-dimensional array with a square grid motif (Fig. 2) presenting the btc^{4-} ligands at the corners, interconnecting the two non-equivalent [Co(pyr)$_4$]$^{2+}$ units located at the edge centres, in a process which involves both atoms Co1 and Co2. The result, presented in Fig. 5, is a neutral tightly bound two-dimensional structure in the form of a 'sieve'.

The way in which the polymeric entities interact with each other in each structure is also different, though mediated in both cases by an extremely complex hydrogen-bonding scheme where all the available donors are active [ten water O—H groups, two pyr N—H groups plus two nonconventional

pyr C—H groups in (I), and four water O—H groups plus four pyr N—H groups in (II); Tables 3 and 4]. The only exception is atom H5WA in (I), which does not have any possible acceptor to interact with (see *Refinement*). The remaining H atoms on atoms O4W and O5W interlink the isolated cationic units having atoms Ni2 as their centres, to define hydrogen-bonded chains running along *b* (Fig. 3b), almost perpendicular to the covalent chains which run along *c*, but shifted half a unit-cell translation along *a*, so that they do not intersect. Figs. 4(a) and 4(b) show views along the *c* direction, with a *c*/2 shift in the vertical direction, suggesting the way in which the voids between covalent chains (Fig. 4a) are 'filled' by the hydrogen-bonded Ni2 chains (Fig. 4b). Hydrogen bonding between the two types of ionic chains stabilizes the structure.

The interplanar interactions in (II) are simpler and are mediated by two solvent water molecules basically interacting with the carboxylate O atoms (Fig. 6). There is, in addition, a π–π bond involving one of the pyr rings [$Cg\cdots Cg(1 - x, -y, 1 - z)$ = 3.74 Å and slippage = 26.66°; Cg is the centroid of the N15/N25/C15/C25/C35 ring]

A survey of the 2009 version of the Cambridge Structural Database (CSD; Allen, 2002) shows that no structures have been published previously containing both the btc anion and the pyr ligand. There are, however, quite a few with the closely related imidazole (imid) group, differing from pyr in that the

two N atoms are not nearest neighbours (positions 1 and 2 in the ring) but next-nearest (positions 1 and 3). In particular, CSD refcode OJOTEM (Cheng *et al.*, 2003), (III), is almost isostructural with (I) in that it presents the equivalent $[Ni(H_2btc)(L)_2(H_2O)_4]_n$ covalent anionic chain counterbalanced by a perpendicular non-intersecting hydrogen-bonded chain made up of water molecules and $[Ni(L)_n(H_2O)_m]^{2+}$ cations, the differences being that in OJOTEM L = imid, m = 2 and n = 4, while in (I) L = pyr, m = 4 and n = 2.

This 'quasi-isostructurality' between complexes (I) and (III), with an almost identical disposition of equivalent groups, ends at and does not include the position of the noncoordinated 'second' N atom (N22) in the five-membered ring. In (I), it occupies site 2, vicinal to the coordinated atom N21 at site 1, a position which forces its H atom (H22) to point inwards within the chain (see Fig. 1), and thus it forms intrachain rather than interchain hydrogen bonds. Its counterpart in OJOTEM, instead, occupies position 3 in the five-membered ring (next-nearest neighbour to the coordinated N atom, the position occupied by atom C12 in Fig. 1), and thus points outwards from the chain in a suitable orientation to act as a donor for strong interchain bonds, which serve to build up hydrogen-bonded two-dimensional structures instead of the basically isolated chains found in (I).

A similar situation arises in (II) where, due to their inward-facing orientation, three out of the four possible N—H groups are forced to make intraplanar hydrogen bonds (Table 4 and Fig. 6) and only the fourth (N25—H25) is involved in the interplanar linkage, *via* a hydrogen-bonding interaction mediated by atom O1*W*.

As a final curiosity resulting from this CSD search, it can be mentioned that the $[Ni(pyr)_2(H_2O)_4]^{2+}$ group in (I) has been reported only once before, its only appearance being in a copper complex (CSD refcode UFIDUI; Wang *et al.*, 2001).

Experimental

An aqueous solution (30 ml) containing Ni(acetate)$_2$·4H$_2$O (0.2985 g) or Co(acetate)$_2$·4H$_2$O (0.2988 g) for (I) and (II), respectively, was added slowly to an aqueous solution (150 ml) containing benzene-1,2,4,5-tetracarboxylic acid (0.1525 g) and NaOH (0.0903 g). The reaction mixture was heated under reflux for 10 min. An ethanolic solution (30 ml) of pyrazole (0.2055 g) was added and the resulting solution was maintained under reflux for 4 h. Single crystals suitable for X-ray crystallography were grown from the solution by slow evaporation at room temperature.

Compound (I)

Crystal data

$[Ni(C_3H_4N_2)_2(H_2O)_4][Ni(C_{10}H_2-$ $O_8)(C_3H_4N_2)_2(H_2O)_2]\cdot 4H_2O$	$\beta = 74.613\ (2)°$
$M_r = 820.02$	$\gamma = 71.287\ (3)°$
Triclinic, $P\bar{1}$	$V = 841.3\ (2)\ \text{Å}^3$
$a = 7.6399\ (12)\ \text{Å}$	$Z = 1$
$b = 10.7925\ (17)\ \text{Å}$	Mo $K\alpha$ radiation
$c = 11.4616\ (19)\ \text{Å}$	$\mu = 1.21\ \text{mm}^{-1}$
$\alpha = 73.224\ (3)°$	$T = 298\ \text{K}$
	$0.28 \times 0.07 \times 0.07$ mm

Table 1
Selected bond lengths (Å) for (I).

Ni1—N12	2.070 (3)	Ni2—O2W	2.059 (2)
Ni1—O1W	2.083 (2)	Ni2—N13	2.068 (3)
Ni1—O31	2.088 (2)	Ni2—O3W	2.076 (2)

Table 2
Hydrogen-bond geometry (Å, °) for (I).

*Cg*2 and *Cg*3 are the centroids of the C31/C11/C21/C31^{iii}/C11^{iii}/C21^{iii} and N13/N23/C13/C23/C33 rings, respectively.

D—H$\cdots A$	D—H	H$\cdots A$	$D\cdots A$	D—H$\cdots A$
N22—H22$\cdots$O21^{i}	0.86	2.04	2.876 (4)	162
N23—H23$\cdots$O5W^{ii}	0.86	2.37	3.216 (5)	168
O1W—H1$WA\cdots$O4W	0.85	1.95	2.798 (3)	172
O1W—H1$WB\cdots$O41^{i}	0.85	1.92	2.679 (3)	148
O2W—H2$WA\cdots$O4W^{ii}	0.85	1.90	2.734 (3)	165
O2W—H2$WB\cdots$O21^{iii}	0.85	1.93	2.759 (3)	165
O3W—H3$WA\cdots$O21^{iii}	0.85	1.97	2.748 (3)	152
O3W—H3$WB\cdots$O11^{iv}	0.85	1.83	2.675 (3)	170
O4W—H4$WB\cdots$O41^{v}	0.85	1.86	2.702 (4)	171
O4W—H4$WA\cdots$O5W^{ii}	0.85	2.31	3.097 (4)	154
O5W—H5$WB\cdots$O11	0.85	2.00	2.809 (4)	159
O5W—H5$WA\cdots Cg2^{vi}$	0.85	2.84	3.64	156
C32—H32$\cdots$O5W^{ii}	0.93	2.44	3.329 (5)	161
C12—H12$\cdots Cg3^{vii}$	0.93	2.92	3.67	140

Symmetry codes: (i) $-x, -y + 1, -z + 2$; (ii) $-x + 1, -y + 1, -z + 1$; (iii) $-x, -y + 1, -z + 1$; (iv) $x, y - 1, z$; (v) $x + 1, y, z$; (vi) $x - 1, y, z$; (vii) $x, y + 1, z - 1$.

Table 3
Selected bond lengths (Å) for (II).

Co1—N13	2.123 (3)	Co2—O41	2.070 (2)
Co1—N12	2.124 (3)	Co2—N14	2.114 (3)
Co1—O21	2.133 (2)	Co2—N15	2.127 (3)

Table 4
Hydrogen-bond geometry (Å, °) for (II).

D—H$\cdots A$	D—H	H$\cdots A$	$D\cdots A$	D—H$\cdots A$
N22—H22$\cdots$O31	0.86	2.12	2.907 (4)	152
N23—H23$\cdots$O11	0.86	1.96	2.806 (4)	166
N24—H24$\cdots$O31	0.86	2.07	2.878 (4)	157
N25—H25$\cdots$O1W	0.86	2.18	2.978 (4)	154
O1W—H1$WA\cdots$O11^{i}	0.85	2.03	2.875 (4)	172
O1W—H1$WB\cdots$O2W	0.85	2.18	2.940 (4)	149
O2W—H2$WA\cdots$O31^{i}	0.85	2.14	2.952 (4)	160
O2W—H2$WB\cdots$O11	0.85	2.21	3.060 (4)	176

Symmetry code: (i) $-x + 1, -y + 1, -z + 1$.

Data collection

Bruker SMART CCD area-detector diffractometer	7155 measured reflections
Absorption correction: multi-scan (*SADABS* in *SAINT-NT*; Bruker, 2002)	3650 independent reflections
	2759 reflections with $I > 2\sigma(I)$
	$R_{int} = 0.030$
$T_{min} = 0.89$, $T_{max} = 0.92$	

Refinement

$R[F^2 > 2\sigma(F^2)] = 0.049$	229 parameters
$wR(F^2) = 0.125$	H-atom parameters constrained
$S = 1.01$	$\Delta\rho_{max} = 0.58$ e Å^{-3}
3650 reflections	$\Delta\rho_{min} = -0.31$ e Å^{-3}

Compound (II)

Crystal data

$[Co_2(C_{10}H_2O_8)(C_3H_4N_2)_8]\cdot 4H_2O$
$M_r = 984.70$
Triclinic, $P\bar{1}$
$a = 8.9122\ (18)$ Å
$b = 11.045\ (2)$ Å
$c = 11.450\ (2)$ Å
$\alpha = 83.381\ (3)°$
$\beta = 74.579\ (3)°$

$\gamma = 74.162\ (3)°$
$V = 1044.1\ (3)$ Å³
$Z = 1$
Mo $K\alpha$ radiation
$\mu = 0.88$ mm^{-1}
$T = 298$ K
$0.42 \times 0.30 \times 0.14$ mm

Data collection

Bruker SMART CCD area-detector
 diffractometer
Absorption correction: multi-scan
 (*SADABS* in *SAINT-NT*;
 Bruker, 2002)
$T_{min} = 0.69$, $T_{max} = 0.89$

8610 measured reflections
4455 independent reflections
3228 reflections with $I > 2\sigma(I)$
$R_{int} = 0.027$

Refinement

$R[F^2 > 2\sigma(F^2)] = 0.053$
$wR(F^2) = 0.123$
$S = 1.04$
4455 reflections

292 parameters
H-atom parameters constrained
$\Delta\rho_{max} = 0.60$ e Å^{-3}
$\Delta\rho_{min} = -0.55$ e Å^{-3}

C-bound H atoms were constrained geometrically and allowed to ride, with C—H = 0.93–0.97 Å. O-bound H atoms were initially found in a difference electron-density map and refined with restrained O—H [0.85 (1) Å] and H···H [1.30 (2) Å] distances until convergence, and then constrained, riding on the host O atoms in the final cycles. In all cases, $U_{iso}(H) = 1.2U_{eq}$(parent).

For both compounds, data collection: *SMART-NT* (Bruker, 2001); cell refinement: *SAINT-NT* (Bruker, 2002); data reduction: *SAINT-NT*; program(s) used to solve structure: *SHELXS97* (Sheldrick, 2008); program(s) used to refine structure: *SHELXL97* (Sheldrick, 2008); molecular graphics: *SHELXTL-NT* (Sheldrick, 2008); software used to prepare material for publication: *SHELXTL-NT* and *PLATON* (Spek, 2009).

References

Ait-Haddou, H., Leedor, M. S. & Gagné, M. R. (2004). *Inorg. Chim. Acta*, **357**, 3854–3864.
Allen, F. H. (2002). *Acta Cryst.* B**58**, 380–388.
Bruker (2001). *SMART-NT*. Version 5.624. Siemens Analytical X-ray Instruments Inc., Madison, Wisconsin, USA.
Bruker (2002). *SAINT-NT*. Version 6.22a (including *SADABS*). Siemens Analytical X-ray Instruments Inc., Madison, Wisconsin, USA.
Cheng, D., Khan, M. A. & Houser, R. P. (2003). *Inorg. Chim. Acta*, **351**, 242–250.
Eddaoudi, M., Moler, D. B., Li, H., Chen, B., Reineke, T. M., O'Keeffe, M. & Yaghi, O. M. (2001). *Acc. Chem. Res.* **34**, 319–330.
Kooijman, H., Spek, A. L., van Albada, G. A., Gamez, P. & Reedijk, J. (2004). *Acta Cryst.* C**60**, m51–m54.
Perron, M. E., Monchamp, F., Duval, H., Boils-Baissier, D. & Wuest, J. D. (2004). *Pure Appl. Chem.* **76**, 1345–1351.
Sheldrick, G. M. (2008). *Acta Cryst.* A**64**, 112–122.
Spek, A. L. (2009). *Acta Cryst.* D**65**, 148–155.
Tudor, V., Marín, G., Kravtsov, V., Simonov, Y. A., Lipkowski, J., Brezeanu, M. & Andruh, M. (2003). *Inorg. Chim. Acta*, **35**, 335–342.
Wang, W.-Z., Liu, X., Liao, D.-Z., Jiang, Z.-H., Yan, S.-P. & Wang, G.-L. (2001). *Inorg. Chem. Commun.* **4**, 327–331.
Yaghi, O. M., Li, H. & Groy, T. L. (1996). *J. Am. Chem. Soc.* **118**, 9096–9101.